Fe^{2+}-Fe^{3+} level as a recombination center in $In_{0.53}Ga_{0.47}As$

B. Srocka, H. Scheffler, and D. Bimberg
Institut für Festkörperphysik, Technische Universitat Berlin, Hardenbergstrasse 36, 10623 Berlin
(Received 13 September 1993; revised manuscript received 2 December 1993)

Thermal emission of electrons and holes from the Fe^{2+}-Fe^{3+} level in $In_{0.53}Ga_{0.47}As$ is investigated in detail. Iron is found to act as a *recombination center* in this material, since majority carrier emission is observed in *n*- and in *p*-type layers. The interaction of the Fe level with free carriers is strongly localized, resulting in statistical distributions of the apparent activation energy and the electron and hole capture cross sections due to the statistical distribution of the occupancy of the cation sites by indium and gallium ions. A detailed general model for carrier capture and emission of a recombination center in a ternary alloy as observed by deep-level transient spectroscopy (DLTS) is developed. The mean energy position of Fe^{2+}-Fe^{3+} is determined as 0.39 ± 0.02 eV above the valence-band edge. This value agrees perfectly with the prediction of the internal reference rule. The electron and hole capture cross sections are distributed over nearly two orders of magnitude, causing a shift of the DLTS peaks with filling pulse width and nonexponential refilling of the traps. The mean values at 250 K are $\sigma_n = 8\pm5\times10^{-18}$ cm^2 and $\sigma_p = 2\pm1\times10^{-17}$ cm^2 for the electron and hole capture cross sections, respectively.

I. INTRODUCTION

$In_{1-x}Ga_xAs$ lattice matched to InP is a widely used material for optoelectronic devices. Because of its high electron mobility it is also suitable for high-speed applications. Layers with semi-insulating characteristics are needed for various $In_{1-x}Ga_xAs$ devices, such as, e.g., for the active region of high-speed metal semiconductor metal photodetectors[1,2] and pin diodes,[3] for device isolation in integrated circuits,[4] and for the channel layer in metal insulator semiconductor–accumulation mode field-effect transistors.[5] Commonly, highly resistive layers are obtained by doping with Fe, which acts as a deep acceptor in III-V semiconductors and hence compensates for a shallow donor background[6–8] usually present in nominally undoped materials.

While the electronic properties of iron in III-V binaries were extensively studied,[9] knowledge about Fe in the ternary $In_{1-x}Ga_xAs$ is much less reliable and complete. The data in the literature concerning the energy position of the Fe^{2+}-Fe^{3+} acceptor level within the band gap vary over a range from 0.35 to 0.46 eV above the valence-band edge.[10] Moreover, capture cross sections for free-carrier capture (σ_n for electrons and σ_p for holes) were not determined directly up to now. To the best of our knowledge, the most complete investigation so far was reported by Guillot *et al.*[11] They observed a resonance peak at 0.34 eV in photoionization experiments. Combining this with results from deep-level transient spectroscopy (DLTS) and photoluminescence (PL) measurements they concluded that this peak is due to the internal $^5E \rightarrow {}^5T_2$ transition of Fe^{2+} followed by the transfer of the excited electron to the conduction band, and, hence, the 0.35-eV apparent activation energy deduced from DLTS belongs to the Fe^{2+}-Fe^{3+} acceptor level.

Due to compositional fluctuations the energetic position of defect levels in semiconductor alloys are commonly treated as distribution functions, which were often assumed to be of Gaussian shape.[12] The capture cross sections even in alloy semiconductors, however, are commonly considered to be well-defined numbers (not distributed). The aim of this paper is to show that for a correct description of the properties of deep impurity levels in a ternary alloy, such as iron in $In_{1-x}Ga_xAs$, broadening mechanisms have to be also considered for the capture cross sections. The recognition that both energy position and carrier capture coefficients are distributed because of the compositional fluctuations of the alloy semiconductor is of fundamental relevance for deep-level investigations in alloys. Moreover, in the interpretation of DLTS experiments charge-carrier emission processes to the conduction band as well as to the valence band must be taken into account. The latter is a direct consequence of the recombination center nature of the level, which is definitely concluded from our experimental results. Thus the former interpretation of the Fe^{2+}-Fe^{3+} level as an electron trap must be revised. Based on our DLTS measurements we will completely determine all electrical parameters of Fe^{2+}-Fe^{3+}, i.e., the distribution functions for the energy position as well as for the capture cross sections, using a sophisticated model which describes the influence of compositional fluctuations on these parameters. The model is suitable not only for the present case but holds generally for all transition-metal-related deep levels in alloy semiconductors. Finally, we will discuss the validity of the internal reference rule[13,14] for the materials GaAs-$In_{1-x}Ga_xAs$-InP, having neither a common anion nor a common cation, based on two transition-metal levels [the Fe^{2+}-Fe^{3+} investigated here together with the recently reported Ti^{3+}-Ti^{4+} (Ref. 15)]. The internal reference rule predicts a constant energy position of the transition metals (TM's) across the heterojunctions with respect to an internal reference level, being the same in all isovalent semiconductors. Thus it allows the precise determination of band discontinuities once the energy positions of the TM's in the various materials are known.

The paper is organized as follows. The experimental procedures are given in the Sec. II, followed by a description of the results in Sec. III. In Sec. IV a detailed model of the impact of alloy broadening on the parameters of a recombination center is presented, which goes far beyond previous models. Here all relevant equations are given which are needed for a simulation of capture and emission processes observed in DLTS. In Sec. V this model will be used to fit the experimental data and distribution functions for the energetic position, and the capture cross sections σ_n and σ_p of the Fe^{2+}-Fe^{3+} level are derived. The results are discussed in Sec. VI. The work is summarized in Sec. VII.

II. CRYSTAL GROWTH AND DIODE FABRICATION

All samples investigated here were grown by liquid-phase epitaxy (LPE) using a conventional sliding boat technique. Growth was carried out from an In solution at a temperature of 635 °C. Indium of 7-N purity, polycrystalline InAs, and GaAs with background carrier concentrations of about 2×10^{16} cm^{-3} and 3-N iron were used as source materials. First, indium and iron were backed at 720 °C for about 100 h for purification from volatile impurities and to ensure complete homogeneity of the iron concentration in the indium. InAs and GaAs were added, and the final solution was again backed at 680 °C for 40 h for further purification. After loading the substrate the system was held at 645 °C for 1 h to homogenize the solution. During this time the InP substrate was covered by another one in order to minimize surface degradation due to phosphorus evaporation.[16] The system was cooled down, and growth was started 3° below the saturation temperature. After 10 min of isothermal growth the samples were cooled rapidly to room temperature. Both *n*- and *p*-type iron-doped layers as well as reference samples without iron were grown with free-carrier concentrations in the range 10^{14}–10^{16} cm^{-3}. The samples with free-carrier concentrations below 10^{15} cm^{-3}, especially prepared for capture DLTS experiments, are obtained using a technique described by Amano.[17] For *p*-type layers, zinc or cadmium doping was used. The distribution coefficient of iron was determined by measuring its concentration in the epitaxial layers by secondary-ion-mass spectroscopy. A value of $3.2\pm0.6\times10^{-4}$ was obtained.

DLTS experiments were carried out on homojunctions formed by the iron-doped layer and a highly doped layer grown on top of it. Additionally, Schottky-diodes were used for DLTS measurements on *p*-type $In_{1-x}Ga_xAs$. For all samples the charge-carrier profiles were measured by electrochemical *C-V* profiling using a Polaron system for *p*/*n*-junction structures or a Hg probe for single layers. This was necessary to confirm the conductivity type in the part of the space-charge region where carrier capture and emission during the DLTS measurements occur. Only LPE-grown structures showing unambiguous carrier profiles were further processed to obtain diodes for the DLTS measurements.

The Schottky diodes on *p*-type $In_{1-x}Ga_xAs$ were fabricated by evaporation of 10-nm titanium followed by 150-nm gold. Just before loading the samples into the evaporation chamber they were etched with $HBr:H_3PO_4:K_2Cr_2O_7$ 1:1:2(0.5*n*) for 20 s in order to remove the surface part of the epilayer, and with HF for another 20 s to keep the native oxide as thin as possible. Dots with diameters of 200, . . . , 800 μm were formed by photolithography and lift-off technique. For the fabrication of ohmic contacts a Ni/Au+Ge/Au sequence was evaporated on *n*-type layers and Ni/Zn/Au on *p*-type layers. The contacts were alloyed at 420 °C for 2 min in a nitrogen atmosphere. Mesa diodes were etched again using $HBr:H_3PO_4:K_2Cr_2O_7$ 1:1:2(0.5*n*) and a finishing etch step with $H_2SO_4:H_2O_2:H_2O$ 1:1:20 (30 sec) to obtain a clean surface. Finally, the mesas were passivated applying a sulfur treatment similar to that reported by Iyler, Bollig, and Lille.[18] Since we produced mesa diodes with diameters up to 800 μm, we got fairly large capacitance signals from the measurements on these devices.

DLTS measurements were performed in a helium-cooled cryostat in the dark. The filling pulses were provided by a Hewlett-Packard HP8115A pulse generator, and the transients were recorded with a Boonton 7200 capacitance meter and a microcomputer. Full isothermal transients taken over a range of temperatures were recorded and stored to generate DLTS boxcar spectra after finishing the temperature scan.

III. EXPERIMENTAL RESULTS

DLTS spectra of the iron acceptor level measured on an *n* and *p*-type $In_{1-x}Ga_xAs$:Fe layers are shown in Fig. 1. For both kinds of materials the respective peaks were not detected in reference samples, where no iron was added to the growth solution. The DLTS peaks are considerably broadened, which is expected from local fluctuations in the chemical composition of the $In_{1-x}Ga_xAs$ layers. The thermal carrier emission characteristics obtained from the Fe-doped layers are depicted in Fig. 2. Our results agree with earlier ones obtained by Guillot *et al.*[11] from measurements on *n*-type $In_{1-x}Ga_xAs$:Fe. Their two uttermost points are reproduced for comparison. Furthermore, within experimental error the thermal sig-

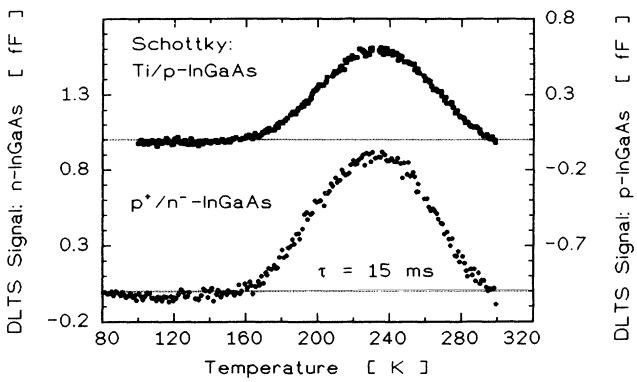

FIG. 1. Electron and hole emission from the Fe^{2+}-Fe^{3+} level in $In_{1-x}Ga_xAs$.

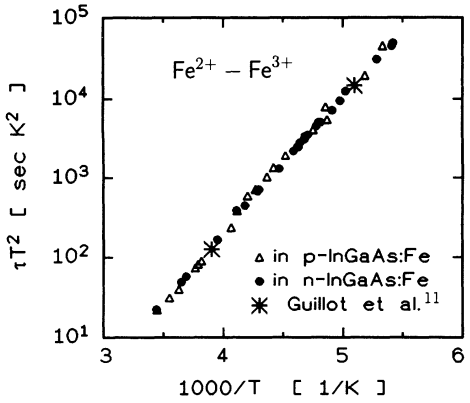

FIG. 2. Arrhenius plots of the thermal emission from the Fe level in n- and p-type $In_{1-x}Ga_xAs$.

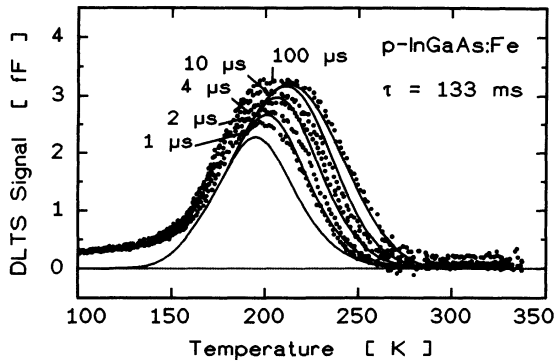

FIG. 4. Filling pulse width dependence of the Fe peak in p-$In_{1-x}Ga_xAs$. Experimental points and fits are shown. ($N_A - N_D$ is 1.5×10^{15} cm^{-3}).

nature measured on p-type layers coincides with the signature obtained from n-type layers. Thus the iron acceptor level is a majority-carrier-emitting trap in n- as well as p-type samples. As a consequence, in the interpretation of DLTS data both emission rates (e_n for electrons and e_p for holes) have to be taken into account, and the slope of the measured emission signature does not yield directly the energetic position of the iron acceptor level within the band gap.[19]

The Arrhenius plots shown in Fig. 2 belong to signals obtained after filling pulses long enough to ensure complete recharging of the traps. This is an important fact, since the peak temperature of the Fe signal in n-type $In_{1-x}Ga_xAs$ increases with the filling pulse width as long as the recharging process has not finished (Fig. 3). A similar effect is also observed in p-type $In_{1-x}Ga_xAs$ as shown in Fig. 4. The low-temperature part of the peak appears first, while the traps contributing to the high-temperature side need a much longer time to become refilled. This observation leads us to conclude that the capture cross sections are distributed due to alloy broadening. The second component contributing to the low-temperature part in the spectrum of n-$In_{1-x}Ga_xAs$:Fe in Fig. 3 is of unknown nature. Since it was not detected in any other sample we deduce that it is not correlated with iron. By performing a differential analysis (subtracting the signal obtained with a pulse as short as 300 ns from all other peaks) we verified that the observed shift of the main peak with pulse width still remains, and is not a result of the overlap of the two components.

In Fig. 5 four DLTS spectra for different emission time constants are shown. The observed increase of peak height with increasing temperature (decreasing time constant) is precisely what we expect for alloy-broadened DLTS peaks.[12]

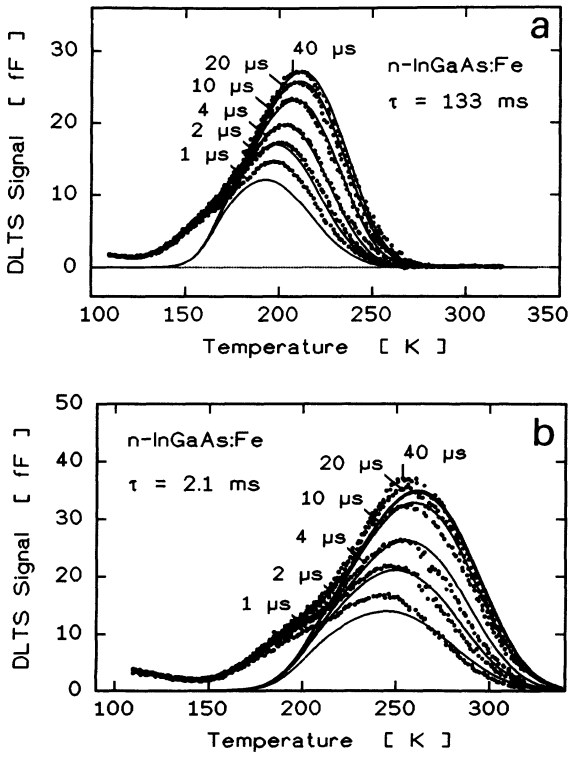

FIG. 3. DLTS signal from the Fe trap after filling pulses of different widths in n-type material. Solid lines show numerical fits (see text). The free-carrier concentration is determined to be 6×10^{14} cm^{-3}.

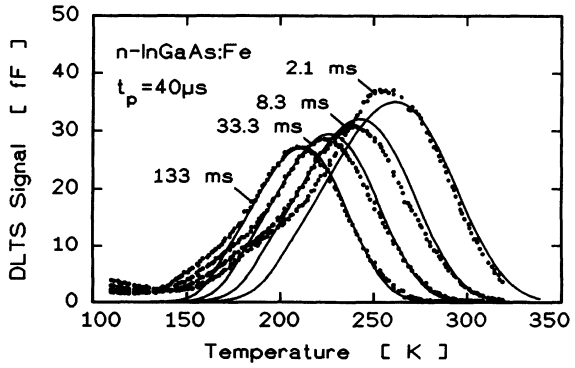

FIG. 5. Fe DLTS peak for different emission time constants in n-type $In_{1-x}Ga_xAs$. The solid lines are the results of the fit as described in the text. ($N_D - N_A$ is 6×10^{14} cm^{-3}).

Finally we have investigated the electrical field dependence of the hole emission rate. There is no measurable influence of the electric field on the emission rate up to a field strength of 1.4×10^5 V/cm, in contrast to what we observed for Ti in InP.[15] Hence field effects are neglected throughout the following considerations.

IV. RECOMBINATION CENTER MODEL FOR THE Fe^{2+}-Fe^{3+} IN THE RANDOM ALLOY $In_{1-x}Ga_xAs$

In DLTS literature, mostly models of ideal electron or hole traps are used for interpreting the experimental results. Since this turns out to be an oversimplification for the iron level under consideration, we will first reexamine the properties of a recombination center.

The rate equation for the occupation probability f_T of the trap can be obtained from simple detailed balance statistics to be

$$\frac{df_T}{dt}=(c_n n+e_p)(1-f_T)-(c_p p+e_n)f_T\ , \tag{1}$$

where e_p and e_n are the hole and electron emission probabilities, c_p and c_n the hole and electron capture coefficients, and p and n the free-carrier concentrations, respectively. Two conclusions can immediately be drawn from Eq. (1). First, the equilibrium occupation probability for the trap is

$$f_T=\frac{e_p+c_n n}{e_p+e_n+c_n n+c_p p}\ , \tag{2}$$

and second, the time constant τ for the complete relaxation of trapped carriers after a small disturbance is

$$\tau=(e_n+e_p+c_n n+c_p p)^{-1}\ . \tag{3}$$

For the space-charge region (excepted for the zone edge where the Debye tail of free carriers has to be considered[19]) p and n are neglectable, and the terms describing the capture processes can thus be disregarded for a first approximation. Moreover for ideal electron or hole traps one can neglect, e.g., for an electron trap, the hole emission. Equation 2 then simply yields the numbers 1 and 0 for the trap occupation under pulse and reverse bias (space-charge region) steady-state conditions in DLTS experiments, respectively.[20] The trap occupation probability then relates directly to the quasi-Fermi-level for electrons F_n. The trap is filled with electrons if it lies energetically below F_n, otherwise it is empty.[21]

The situation changes if both emission probabilities e_n and e_p are of the same order of magnitude. Then the occupation probability of the trap is not simply connected to one of the quasi-Fermi-levels, since both types of charge carriers participate in the emission and capture processes of the trap. The trap will be only partly recharged during reverse bias, reaching an equilibrium occupation $f_T=e_p/(e_n+e_p)$ for neglectable free-carrier concentrations [see Eq. (2)]. Thus f_T is now a number *between* 0 and 1. Hence one may observe such a recombination center in both n- and p-type materials as a majority-carrier-emitting trap. And, vice versa, a level which is observed in n- and p-type materials as a majority-carrier-emitting trap must be a recombination center. This is indeed the case for the Fe^{2+}-Fe^{3+} in $In_{1-x}Ga_xAs$, as shown in Figs. 1 and 2. As a second consequence, the time constant τ observed for the emission in both materials is now the inverse of the sum of e_n and e_p. Therefore the plot of τT^2 versus $1/T$ is no longer a simple logarithmic function of the activation energy of the trap with respect to one band edge. One obtains

$$\tau^{-1}=e_n+e_p$$
$$=c_n\gamma N_c\exp\left[\frac{E_T-E_G}{kT}\right]+c_p\gamma^{-1}N_V\exp\left[-\frac{E_T}{kT}\right]\ , \tag{4}$$

where E_T is the energetic position of the trap measured from the valence-band edge, and γ denotes the ratio of the degeneracy of the empty trap to that of the filled one. N_C and N_V are the conduction- and valence-band effective densities of states, respectively. Different sets of parameters E_T, c_n and c_p will now satisfy the same Arrhenius plot, and, hence, a calculation of the correct activation energy from such a plot alone is not possible. Since the two exponential terms in Eq. (4) are at least weighted by the capture cross sections, it is necessary to determine the carrier capture cross sections independently by measuring the DLTS signal after filling pulses of different widths.[20]

Performing these experiments, another difficulty appears in the ternary alloy material $In_{1-x}Ga_xAs$. As is well known, the peaks in DLTS spectra are usually considerable broadened due to the spatially fluctuating composition of alloy semiconductors.[22] Depending on the occupation of the cation sites next to the impurity by In or Ga, different impurity ions may have different trap energies and capture cross sections. While to a first approximation the inclusion of a Gaussian broadening of the activation energy may be thought to be sufficient, considering the filling pulse width dependence of the signals demonstrates that this picture is too simple. In general, the capture cross sections σ_n and σ_p also have to be considered as distributed over a distinct range.[23] Only this extension of the model can explain the peak shift to higher temperatures with increasing filling pulse width, shown in Figs. 3 and 4. The traps with larger cross sections within the distribution contribute mainly to the low-temperature side of the DLTS peak, according to Eq. (4). Since these traps are recharged faster during the filling pulse, the low-temperature part of the peak will appear first. The traps having smaller cross sections, contributing mainly to the high-temperature part of the peak, need more time to be recharged, and hence this peak side appears last.

For a recombination center, we have at least three parameters—E_T, σ_n and σ_p— which obey a distribution function due to the compositional fluctuation of the ternary alloy $In_{1-x}Ga_xAs$ (or analogous other alloys). Therefore, we have to consider the distribution of the cation, and must derive the resulting distributions for the three parameters needed here. Such a calculation was done for photoluminescence experiments by Schubert *et al.*[24] They pointed out that the standard deviation σ_x

of the alloy composition x within a distinct volume V_{trans} is given by the binomial distribution

$$\sigma_x = \left[\frac{x(1-x)}{KV_{\text{trans}}} \right]^{1/2} . \quad (5)$$

Here K stands for the cation density, while V_{trans} is the characteristic volume of the transition under consideration (e.g., for excitonic PL lines the exciton volume). In order to obtain the corresponding standard deviation for a quantity Y one has to multiply σ_x with the derivative dY/dx (e.g., for the excitonic transition dE_G/dx). If the volume V_{trans} is large enough, one may approximate the binomial by a Gaussian distribution. Unfortunately this ansatz cannot be used in our case, since the characteristic volume V_{trans} is not known. From, e.g., the capture cross sections themselves, one cannot directly calculate this volume since the corresponding radii r_σ are normally smaller than half a lattice constant (for a trap with $\sigma_n = 1\times10^{-15}$ cm^2, $r_\sigma \approx 1.8$ Å), and hence the volume, thus obtained, does not contain any cation at all. A closer look reveals that, e.g., in order to modify the activation energy, we need to know how many shells of cations influence the potential of the trap. Moreover, this potential is a function of the cation distance to the trap and of the local symmetry, i.e., especially of the arrangement of the different cations. From this point of view Eq. (5) is too simple.

We will use a different model to describe results, which will be explained with the help of Fig. 6, where the x dependence of the relevant energies is shown. The valence-band position is defined by three points: the position of the InAs and $In_{1-x}Ga_xAs$ valence bands with respect to GaAs. The resulting bowing is approximated by a parabolic curve. Since the available data for the InAs/GaAs band offset scatter appreciably, one must treat them as adjustable parameters within a certain range. Values ranging from -0.1 to $+0.35$ eV are reported.[13,25–28] For the valence-band offset between $In_{1-x}Ga_xAs$ and GaAs we took the value of 0.17 eV derived from the Ti^{3+}-Ti^{4+} level position in these materials.[15] The conduction-band energy is determined using the relation for the band gap given by Goetz *et al.*,[29] and the temperature dependence after Louati *et al.*[30] It is assumed that the relative band offsets do not change with temperature.

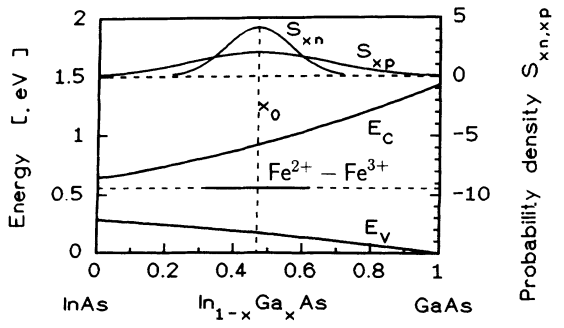

FIG. 6. Band-edge variation and distribution functions used in the calculations (see text).

The energy position E_T of the trap within the forbidden gap is measured from the valence-band edge. The cross sections σ_n and σ_p and, hence, the capture coefficients c_n and c_p of the trap, are given by[31]

$$c_{n,p} = \sigma_{n,p} v_{n,p}^{\text{th}} = \sigma_{n,p}^{\infty} \left[\frac{3kT}{m_{e,h}^*} \right]^{1/2} \exp\left[-\frac{E_{\sigma n,\sigma p}}{kT} \right] \quad (6)$$

where σ_n^∞ and σ_p^∞ are the capture cross sections at infinite temperature with their respective activation energies $E_{\sigma n}$ and $E_{\sigma p}$. The degeneracy ratio γ in Eq. (4) is calculated in agreement with the level splitting of the free Fe^{2+} ion in the tetraedric symmetry of the crystal field.[32]

All these values are first calculated for $In_{1-x}Ga_xAs$ lattice matched to InP. The alloy broadening is now allowed for by Gaussian distributions for E_T, $E_G - E_T$, σ_n, and σ_p. Since the wave functions forming the valence and conduction bands are of different types, different characteristic volumes for the interactions of the trap with the two bands may eventually result. We therefore assume to a first approximation two couplet Gaussian distributions of possibly different widths (standard deviations are S_{xp} and S_{xn}), one in each case for interactions with the valence (E_T and σ_p) and conduction ($E_G - E_T, \sigma_n$) bands, respectively. The energetic position of the iron level does not depend on x, according to the predictions of the internal reference rule.[13] The variation of the trap energy is thus directly obtained from the variation of the band-edge positions with x. The capture cross sections σ_n and σ_p are assumed to vary exponentially with x. We approximate them by $\sigma_{n,p} = \exp(a_{n,p}x^2 + b_{n,p}x + c_{n,p})$, matching the values in InAs, $In_{1-x}Ga_xAs$, and GaAs, which are taken as fit parameters. Their activation energies are kept constant for the sake of simplicity. For each x value within the two Gaussian distributions, Eqs. (2)–(4) can be used. In, e.g., an n-type semiconductor, for the occupation probability f_T within the emission region when the bias voltage is applied (see the Appendix), one obtains

$$f_T(x,t) = 1 - \frac{e_n(x)}{e_n(x)+e_p(x)} \times \left(1 - \{1 - \exp[-\sigma_n(x) n_0 v_{\text{th}} t_p]\} \times \exp\{1 - t[e_n(x)+e_p(x)]\}\right) . \quad (7)$$

There t_p is the filling pulse width. The contribution of the traps at each x to the capacitance change is thus computed[20,33] and weighted by the Gaussian distributions. The Debye tail is also taken into account, as well as effects resulting from incomplete discharging of traps at low temperatures due to finite measuring times (see the Appendix). Summing up over all x values, one obtains the signal produced by the whole trap population. Performing this procedure at several temperatures, we can simulate the DLTS boxcar spectrum, containing all information available from the measurement.

The thermalization of free carriers into the potential valleys formed by the fluctuating band edges is also in-

cluded in the model. This relaxation is observed, e.g., in photoluminescence experiments.[34,35] Since the relaxation time of the free carriers is much shorter than the capture times, one can account for this effect simply by a Boltzmann distribution of the carriers in potentials $\Delta E_{C,V}(x)$. Since free carriers average over a distinct volume, this energy is damped by a factor α. We finally obtain, e.g., for the electron concentration,

$$n(x)=n_0 \exp\left[-\frac{\alpha \Delta E_c(x)}{kT}\right]. \quad (8)$$

This effect influences the capture processes, since electron density at Fe traps having an In-rich surrounding is larger than at Fe traps with a Ga-rich surrounding.

V. NUMERICAL ANALYSIS

Although the number of parameters required to describe the experiments is quite large, our model is still approximate, since second-order effects (such as, e.g., a different temperature dependence for σ_n and σ_p in $In_{1-x}Ga_xAs$, InAs, and GaAs) are neglected to keep the number of parameters as small as possible. Moreover, some assumptions have also only approximate character. For example, the temperature dependence of the trap energy was never investigated to the best of our knowledge.

Using the same broadening parameters for electron and hole processes ($S_{xn}=S_{xp}$), a simulation of all experimental results in n- and p-type layers is not possible. This can be understood in terms of the very different slopes of the conduction- and valence-band variations with x. Since the conduction band varies much faster with x than the valence band, the standard deviation necessary to explain the width of the observed peaks is much smaller in n-type layers than in p-type ones. Note that this difference comes not from the time emission constant τ [see Eq. (3)], since τ is equal for every trap at a distinct x value in both materials. The real reason for the different behavior is the weighting of the variation in occupation probabilities by the emission probabilities themselves [see Eqs. (A3) and (A4)]. Second, the thermalization of free carriers into the potential valleys of the bands was found to be essential for the time dynamic of the signal. Without the consideration of this effect, it is not possible to explain the fast filling of the traps producing the low-energy side of the DLTS peak. This is a little bit surprising, since these levels are already refilled faster due to their larger capture cross sections than are other ones. But it is only in connection with the enhancement of their capture rate by the thermalization mentioned above that the observed fast recharging of these traps is sufficiently accounted for in the simulation.

The broadening parameters which we obtain from experiment are in qualitative agreement with the standard deviation of a binomial distribution accounting for the 12 next cationic neighbors of the iron atom in the crystal, yielding $\sigma_x=0.144$. This fact shows that indeed to a first approximation only these 12 next neighbors have to be taken into account.

The parameter set of our best fit to the data is listed in Table I. With this set a satisfactory fit could be obtained, as is shown in Figs. 3–5. Figure 7 and 8 show the resulting distributions of the relevant parameters E_T, E_G-E_T, σ_n, and σ_p.

VI. DISCUSSION

The mean value of the energy distance of 0.39 ± 0.02 eV of the Fe level from the valence band describes well

TABLE I. Best-fit parameters for modeling the thermal emission of the Fe^{2+}-Fe^{3+} level in $In_{1-x}Ga_xAs$.

Parameter	Value
Trap energy E_T-E_V at 300 K	0.39 ± 0.02 eV
Capture cross section σ_n for electrons at 250 K:	
in $In_{1-x}Ga_xAs$	$8\times10^{-18}\pm5\times10^{-18}$ cm^2
GaAs	$1\times10^{-19}\pm5\times10^{-20}$ cm^2
InAs	$1\times10^{-14}\pm5\times10^{-15}$ cm^2
Activation energy $E_{\sigma n}$ of σ_n:	80±30 meV
Capture cross section σ_p for holes at 250 K:	
in $In_{1-x}Ga_xAs$	$2\times10^{-17}\pm1\times10^{-17}$ cm^2
GaAs	$4\times10^{-16}\pm2\times10^{-16}$ cm^2
InAs	$1\times10^{-17}\pm5\times10^{-18}$ cm^2
Activation energy $E_{\sigma p}$ of σ_p:	−40±20 meV
Standard deviation of the Gaussian distributions	
Electron processes S_{xn}	0.1±0.03
Hole processes S_{xp}	0.2±0.05
Valence-band offsets: $E^V_{In_{1-x}Ga_xAs}/E^V_{GaAs}$	0.17±0.03 eV
E^V_{InAs}/E^V_{GaAs}	0.28±0.05 eV

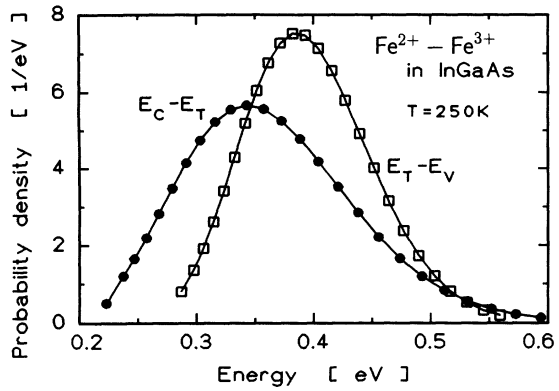

FIG. 7. Distributions of the energy distances between the Fe level and the band edges.

the free-carrier concentration as a function of Fe doping in $In_{0.53}Ga_{0.47}As$ (see Fig. 9). The value coincides with the results of temperature-dependent Hall measurements.[7] The explanation given by Guillot *et al.*[11] for their observation of a resonance peak at about 0.34 eV in the photoionization cross-section curve is also in agreement with our result. According to the crystal-field splitting of 0.35 eV between the ^5E ground and the $^5T_2$ excited states, the carriers, optically excited to the $^5T_2$ level, must at least overcome the 30-meV rest to enter the conduction band (at the temperature of the photoionization measurements—82 K—we calculate for the Fe-ground state to be at a distance of 0.38 eV from the conduction band according to the assumption of proportionality between level position and band gap variation with temperature). Thermal as well as a second optical excitation may be responsible for this step. It is clear that the only level investigated in DLTS experiments is the ^5E ground level of the Fe^{2+} charge state, since, e.g., in an n-type layer the iron is just in this state after the filling pulse was applied. A signal caused by thermal excitation of an electron to the $^5T_2$ level eventually occurring under bias will always be covered by the strong broadening of the observed DLTS peaks. Finally Fig. 10 shows a comparison of the Fe^{2+}-Fe^{3+} level in GaAs, InP and $In_{1-x}Ga_xAs$. Here we used the band discontinuities derived from the Ti^{3+}-Ti^{4+} level positions within these materials.[15] For the Fe level in GaAs and InP, we took the data from Klevermann *et al.*[36] and Juhl *et al.*,[37] respectively. Obviously the Fe^{2+}-Fe^{3+} energies agree with the predictions of the internal reference rule[13] within ± 20 meV. This observation substantiates that the internal reference rule is a powerful tool for the determination of heterojunction band discontinuities.

The InAs/GaAs valence-band offset giving the best fit to our data (see Fig. 6) is in agreement with predictions by Langer *et al.*[13] and Kroemer,[27] and disagrees with positions calculated in Refs. 25 and 26. A detailed discussion of this result is enclosed in Ref. 13. Following the internal reference rule we can now predict the energy of the Fe^{2+}-Fe^{3+} level in InAs to be at about 0.09 eV below the conduction band. This seems to contradict the results of Huang and Wessels,[38] who investigated the iron level in $InAs_xP_{1-x}$ for x values up to 0.5. They predicted the iron level to be just in resonance with the conduction band in InAs. However, the deduction of the energy position of the Fe level from the temperature dependence of the resistivity as in Ref. 38 is in our opinion not a proper method, since the mobility is also a function of the temperature. Additionally, the bowing of the $InAs_xP_{1-x}$ band gap is not included in the calculation presented there (the bowing parameter in the literature varies between 0.16 and 0.32 eV).

The electron capture cross section in GaAs matches the value derived by Klevermann *et al.*[36] and Lang and Logan.[39] In the ternary $In_{1-x}Ga_xAs$ it varies inversely with the distance of the Fe level from the conduction band edge (see Table I and Fig. 6). This tendency agrees qualitatively with the model of multiphonon emission.[21,31] The observed temperature dependence of the capture cross section is also expected from such an emission model.[31] The matrix dependence of the hole capture cross section is completely different. While for GaAs it again matches the previously found value,[39] it drops with increasing indium content (decreasing E_T). In fact, we do not observe a DLTS signal in n-type $In_{1-x}Ga_xAs$ layers if we assume a higher value of the hole capture cross section than in GaAs. In order to explain the measured

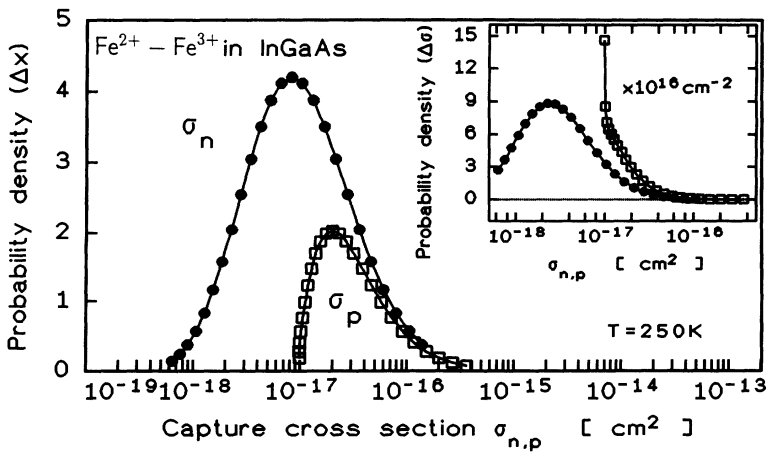

FIG. 8. Capture cross-section distributions. Although in the main picture the probability density is depicted vs the cross sections, it is normalized with respect to x. The inset shows the same distributions normalized to the capture cross sections themselves.

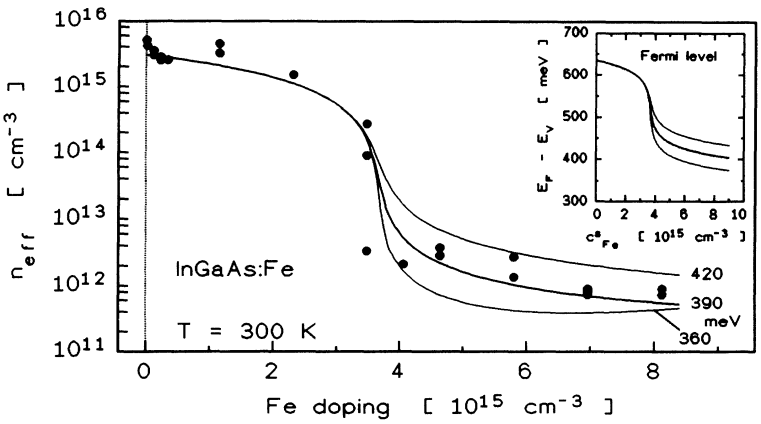

FIG. 9. Carrier concentration vs iron-doping level. The solid lines are the result of a numerical calculation with the trap energy above the valence-band edge, as a parameter indicated on the right. The inset shows the resulting Fermi-level variation.

data, we definitely need a lower value, and an even lower one on the In-rich side. This tendency as well as the small decreases of σ_p with increasing temperature seems to contradict a multiphonon emission. Therefore the dominant capture mechanism for holes may be of a different type.

VII. CONCLUSIONS

We have investigated in detail the thermal emission of carriers from the Fe^{2+}-Fe^{3+} level in $In_{1-x}Ga_xAs$ using DLTS. The iron acceptor level is found to act as a recombination center, having comparable emission probabilities for electrons and holes. The former interpretation as an electron trap must therefore be revised. The observation of the level in n- and p-type materials as a majority carrier-emitting trap is definite proof of this characteristic. This behavior is in agreement with iron acting as a hole trap in GaAs, while in InAs it is predicted to be near or in resonance to the conduction-band edge and therefore should act as an electron trap.[38] Thus the recombination center characteristics of the iron level observed in $In_{1-x}Ga_xAs$ represents the transition between two extreme trap properties in the two binaries.

The emission characteristic is simulated with the help of a sophisticated model accounting for the recombination center nature of the level, as well as for alloy broadening effects. Interaction of the level with free carriers is found to be strongly localized. This results in a considerable broadening of the DLTS peaks, nonexponential carrier capture and emission, temperature shift of the peak with the filling pulse width, and increasing peak height with the emission time constant. The energetic position and capture cross sections are distributed over a considerable range instead of being well-defined numbers caused by a Gaussian distribution of the composition fluctuations. Their distribution functions are explicitly given. The model developed by us is of general relevance, since it is in principle suitable for any transition-metal-related deep level in semiconductor alloys.

The mean value of the energy position of the Fe^{2+}-Fe^{3+} level is determined to be 0.39 ± 0.02 eV above the valence-band edge at room temperature. Following the internal reference rule one obtains from this value the same band offsets for InP and GaAs as from the Ti^{3+}-Ti^{4+} level.[15] Using this rule the Fe level in InAs is expected to lie about 0.09 eV below the conduction-band edge.

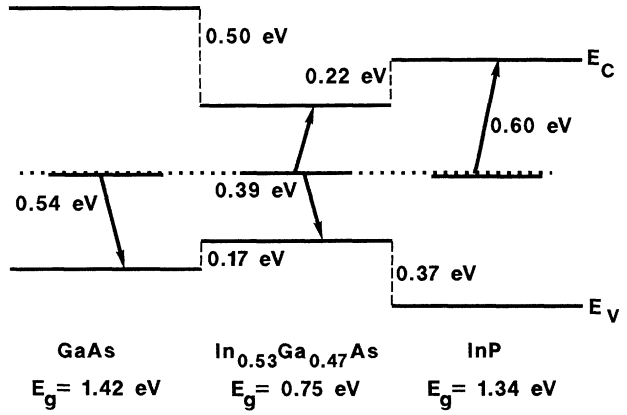

FIG. 10. Fe^{2+}-Fe^{3+}-level position in GaAs, $In_{1-x}Ga_xAs$, and InP at 300 K. The band offsets are taken from Ref. 15.

APPENDIX

Under bias the equilibrium occupation f_0 within the main emission region (except the edge of the space-charge region, where Debye-tail effects must be taken into account) is

$$f_0=\frac{e_p}{e_n+e_p}\ . \tag{A1}$$

This holds for n- and p-type backgrounds. After the bias voltage is applied for a long enough time t_b to allow all traps to reach equilibrium, for the occupation probability f_T^p at the end of the filling pulse of width t_p, one obtains, e.g., in an n-type layer,

$$\begin{aligned} f_T^p &= 1+(f_0-1)\exp(-c_n n_0 t_p) \\ &= 1-\frac{e_n}{e_n+e_p}\exp(-\sigma_n n_0 v_{\rm th} t_p)\ . \end{aligned} \tag{A2}$$

Reemission processes are neglected here. Since the trap under consideration is deep and trap concentrations are

small compared to those of the shallow dopants, the equilibrium occupation in the bulk is assumed to be 1. Hence, for the recharging after bias is applied again, we obtain

$$f_{Tn}^{b}(t)=f_0+(f_T^p-f_0)\exp[-t(e_n+e_p)]$$
$$=1-\frac{e_n}{e_n+e_p}\{1-[1-\exp(-\sigma_n n_0 v_{\rm th} t_p)]\times\exp[-t(e_n+e_p)]\}\ . \quad \text{(A3)}$$

For a p-type background the occupation probability for holes is

$$f_{Tp}^{b}(t)=1-\frac{e_p}{e_n+e_p}\{1-[1-\exp(-\sigma_p p_0 v_{\rm th} t_p)]\times\exp[-t(e_n+e_p)]\}\ . \quad \text{(A4)}$$

Note that the time dependence of the emission is the same for both background types, while the prefactors are different.

Considering that at low temperatures the traps cannot reach the equilibrium f_0 during the bias until the next pulse is applied, one realizes that the trap density may be overestimated by computing a boxcar spectrum. If the filling pulse is long enough to refill all traps, this effect vanishes. Otherwise, for incomplete refilling, e.g., in filling pulse-width-dependent measurements, an equilibrium develops between refilled and discharged traps during pulse t_p and bias t_b, respectively. Setting

$$\Psi_p=\exp(-t_p/\tau_p)=\exp[-t_p c_n n_0] \quad \text{(A5a)}$$

and

$$\Psi_b=\exp(-t_b/\tau_b)=\exp[-t_b(e_n+e_p)]\ , \quad \text{(A5b)}$$

where τ_p and τ_b are capture and emission time constants, respectively, for the occupation in an n-type layer at the end of the pulse one obtains

$$f_{p,t_p}=(1-f_{b,t_b})(1-\Psi_p)+f_{b,t_b} \quad \text{(A6)}$$

and, at the end of the bias,

$$f_{b,t_b}=(f_{p,t_p}-f_0)\Psi_b+f_0\ . \quad \text{(A7)}$$

Introducing Eq. (A7) into (A6) at the end of the pulse we obtain

$$f_{p,t_p}=\frac{(1-\Psi_p)+f_0(1-\Psi_b)\Psi_p}{1-\Psi_b\Psi_p}\ . \quad \text{(A8)}$$

This relation has to be used instead of Eq. (A2) under the circumstances mentioned. For a p-type layer a similar relation holds if one considers the hole occupation probability and uses $f_{p0}=1-f_0$ instead of f_0.

[1]E. H. Böttcher, D. Kuhl, F. Hieronymi, E. Dröge, T. Wolf, and D. Bimberg, IEEE Quantum. Electron. **QE-28**, 2343 (1992).

[2]D. Kuhl, F. Hieronymi, E. H. Böttcher, T. Wolf, A. Krost, and D. Bimberg, Electron. Lett. **26**, 2107 (1990).

[3]V. Diadiuk and S. H. Groves, Appl. Phys. Lett. **46**, 157 (1985).

[4]H. Matsuda, T. Tanaka, and M. Nakamura, in *Semiconductors and Semimetals,* edited by R. K. Willardson and A. C. Beer (Academic, New York, 1990), Vol. 30, Chap. 6.

[5]H. H. Wieder, J. L. Veteran, A. R. Clawson, D. P. Mullin, and D. I. Elder, Appl. Phys. Lett. **43**, 287 (1983).

[6]M. Kondo, M. Sugawara, T. Tanahashi, S. Isozumi, and K. Nakajima, Appl. Phys. Lett. **53**, 574 (1988).

[7]B. Tell, U. Koren, and B. I. Miller, J. Appl. Phys. **61**, 1172 (1987).

[8]S. H. Groves, V. Diadiuk, M. C. Plonko, and D. L. Hovey, Appl. Phys. Lett. **46**, 78 (1985).

[9]S. G. Bishop, in *Deep Centers in Semiconductors,* edited by S. T. Pantelides (Gordon and Breach, New York, 1986), Chap. 8.

[10]D. Bimberg and B. Srocka, in *Properties of Lattice-Matched and Strained* $In_{1-x}Ga_xAs$, edited by P. Bhattacharya, EMIS Datareviews Series No. 8 (Inspec, London, 1993), p. 162.

[11]G. Guillot, G. Bremond, T. Benyattou, F. Ducroquet, B. Wirth, M. Colombet, A. Louati, and A. Bencherifa, Semicond. Sci. Technol. **5**, 391 (1990).

[12]P. Omling, L. Samuelson, and H. G. Grimmeiss, J. Appl. Phys. **54**, 5117 (1983).

[13]J. M. Langer, C. Delerue, M. Lannoo, and H. Heinrich, Phys. Rev. B **38**, 7723 (1988).

[14]M. Hamera, W. Walukiewicz, D. D. Nolte, and E. E. Haller, Phys. Rev. B **39**, 10 114 (1989).

[15]N. Baber, H. Scheffler, A. Ostmann, T. Wolf, and D. Bimberg, Phys. Rev. B **45**, 4043 (1992).

[16]B. Sartorius, M. Schlak, M. Rosenzweig, and K. Pärschke, J. Appl. Phys. **63**, 4677 (1988).

[17]T. Amano, S. Kondo, and H. Nagai, Jpn. J. Appl. Phys. **31**, 2185 (1992).

[18]R. Iyler, B. Bollig, and D. L. Lille, in *IEEE Third International Conference on Indium Phosphide and Related Materials, Cardiff, UK,* edited by T. Ridley (IEEE, New York, 1991), p. 621.

[19]G. M. Martin, A. Mitonneau, D. Pons, A. Mircea, and D. W. Woodard, J. Phys. C **13**, 3855 (1980).

[20]A. C. Wang and C. T. Sah, J. Appl. Phys. **57**, 4645 (1985).

[21]J. Bourgoin and M. Lannoo, *Point Defects in Semiconductors II,* Springer Series in Solid State Science Vol. 35 (Springer, Berlin, 1983), Chap. 6.

[22]L. Samuelson, in *13th International Conference on Defects in Semiconductors, Coronado, California, 1984,* edited by L. C. Kimerling and J. M. Parsey, Jr. (AIME, New York, 1984), p. 101.

[23]M. Kaniewska and J. Kaniewski, Solid State Commun. **53**, 485 (1985).

[24]E. F. Schubert, E. O. Göbel, Y. Horikoshi, K. Ploog, and H. J. Queisser, Phys. Rev. B **30**, 813 (1984).

[25]S. Tiwari and D. J. Frank, Appl. Phys. Lett. **60**, 630 (1992).

[26]R. S. Bauer and G. Margaritondo, Phys. Today **40** (1), 27 (1987).

[27]H. Kroemer, J. Vac. Sci. Technol. B **2**, 433 (1984).

[28]S. P. Kowalczyk, W. J. Schaffer, E. A. Kraut, and R. W. Grant, J. Vac. Sci. Technol. **20**, 705 (1982).

[29]K.-H. Goetz, D. Bimberg, H. Jürgensen, J. Selders, A. V. Solomonov, G. F. Glinskii, and M. Razeghi, J. Appl. Phys. **54**, 4543 (1983).

[30]A. Louati, C. Charreaux, A. Nouailhat, G. Guillot, P. N.

Favennec, and M. Salvi, Solid State Commun. **62**, 31 (1987).
[31]C. H. Henry and D. V. Lang, Phys. Rev. B **15**, 989 (1977).
[32]H. L. Schäfer and G. Gliemann, *Einführung in die Ligandenfeldtheorie* (Akademische Verlagsgesellschaft, Frankfurt, 1967).
[33]D. S. Day, M. Y. Tsai, B. G. Streetman, and D. V. Lang, J. Appl. Phys. **50**, 5093 (1979).
[34]J. Christen and D. Bimberg, Phys. Rev. B **42**, 7213 (1990).
[35]R. F. Schnabel, R. Zimmermann, D. Bimberg, H. Nickel, R. Lösch, and W. Schlapp, Phys. Rev. B **46**, 9873 (1992).
[36]M. Klevermann, P. Omling, L. Å. Ledebo, and H. G. Grimmeiss, J. Appl. Phys. **54**, 814 (1983).
[37]A. Juhl, A. Hoffmann, D. Bimberg, and H. J. Schulz, Appl. Phys. Lett. **50**, 1292 (1987).
[38]K. Huang and B. W. Wessels, J. Appl. Phys. **64**, 6770 (1988).
[39]D. V. Lang and R. A. Logan, J. Electron. Mater. **4**, 1053 (1975).